

SECOND EDITION

Characterization of **MATERIALS**

Volume 2

EDITED BY

Elton N. Kaufmann

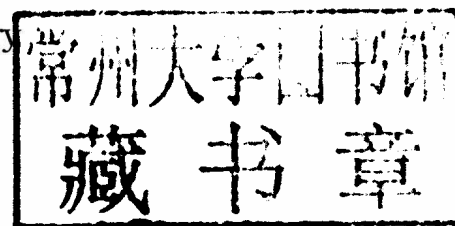
CHARACTERIZATION OF MATERIALS

SECOND EDITION

Volume 2

Editor-in-Chief

Elton N. Kaufmann
Argonne National Laboratory



Characterization of Materials is available Online in full color
at www.mrw.interscience.wiley.com/com.

A JOHN WILEY & SONS, INC., PUBLICATION

Copyright © 2012 by John Wiley & Sons, Inc. All rights reserved.

Published by John Wiley & Sons, Inc., Hoboken, New Jersey.
Published simultaneously in Canada.

No part of this publication may be reproduced, stored in a retrieval system, or transmitted in any form or by any means, electronic, mechanical, photocopying, recording, scanning, or otherwise, except as permitted under Section 107 or 108 of the 1976 United States Copyright Act, without either the prior written permission of the Publisher, or authorization through payment of the appropriate per-copy fee to the Copyright Clearance Center, Inc., 222 Rosewood Drive, Danvers, MA 01923, (978) 750-8400, fax (978) 750-4470, or on the web at www.copyright.com. Requests to the Publisher for permission should be addressed to the Permissions Department, John Wiley & Sons, Inc., 111 River Street, Hoboken, NJ 07030, (201) 748-6011, fax (201) 748-6008, or online at <http://www.wiley.com/go/permission>.

Limit of Liability/Disclaimer of Warranty: While the publisher and author have used their best efforts in preparing this book, they make no representations or warranties with respect to the accuracy or completeness of the contents of this book and specifically disclaim any implied warranties of merchantability or fitness for a particular purpose. No warranty may be created or extended by sales representatives or written sales materials. The advice and strategies contained herein may not be suitable for your situation. You should consult with a professional where appropriate. Neither the publisher nor author shall be liable for any loss of profit or any other commercial damages, including but not limited to special, incidental, consequential, or other damages.

For general information on our other products and services or for technical support, please contact our Customer Care Department within the United States at (800) 762-2974, outside the United States at (317) 572-3993 or fax (317) 572-4002.

Wiley also publishes its books in a variety of electronic formats. Some content that appears in print may not be available in electronic formats. For more information about Wiley products, visit our web site at www.wiley.com.

Library of Congress Cataloging-in-Publication Data:

Characterization of materials / edited by Elton N. Kaufmann, Argonne National Laboratory,
Argonne, IL. – Second edition.

volumes cm

First edition published as a two volume set, ©2003.

Includes bibliographical references and index.

ISBN 978-1-118-11074-4 (3 volume set)

1. Materials—Research. 2. Materials—Testing. I. Kaufmann, Elton N.

TA404.2.C48 2012

620.1'10287—dc23

2012012521

Printed in the United States of America

10 9 8 7 6 5 4 3 2 1

CHARACTERIZATION OF MATERIALS

EDITOR-IN-CHIEF

Elton N. Kaufmann

Argonne National Laboratory
Argonne, IL

CHAPTER EDITORS

Reza Abbaschian

University of California
Riverside, CA

Peter A. Barnes

Clemson University
Clemson, SC

Andrew B. Bocarsly

Princeton University
Princeton, NJ

Chia-Ling Chien

Johns Hopkins University
Baltimore, MD

Lawrence P. Cook

The Catholic University of America
Washington DC

Alan I. Goldman

Iowa State University
Ames, IA

Joseph P. Hornak

Rochester Institute of Technology
Rochester, NY

Chris Jeynes

University of Surrey
Guildford, UK

Stephen J. Pennycook

Oak Ridge National Laboratory
Oak Ridge, TN

Alan C. Samuels

Edgewood Chemical Biological Center
Aberdeen Proving Ground, MD

Juan M. Sanchez

The University of Texas at Austin
Austin, TX

Alexander Schwarz

Universität Hamburg
Hamburg, Germany

EDITORIAL STAFF

VP & Director, STMS Book Publishing: Janet Bailey

Executive Editor: Arza Seidel

Development Editor: Mihai Peterca

Production Manager: Shirley Thomas

Production Editor: Kristen Parrish

Illustration Editor: Dean Gonzalez

CONTENTS, VOLUMES 1, 2, AND 3

FOREWORD TO THE SECOND EDITION	ix	Dynamical Diffraction	318
FOREWORD TO THE FIRST EDITION	xi	Computation of Diffuse Intensities in Alloys	346
PREFACE	xiii	MECHANICAL TESTING	377
CONTRIBUTORS	xvii	Mechanical Testing, Introduction	379
COMMON CONCEPTS	1	Tension Testing	379
Common Concepts in Materials		High-Strain-Rate Testing of Materials: The	
Characterization, Introduction	3	Split-Hopkinson Pressure Bar	390
General Vacuum Techniques	3	Fracture Toughness Testing Methods	404
Mass and Density Measurements	29	Hardness Testing	420
Porosity and Its Measurement	35	Tribological and Wear Testing	429
Thermometry	44	Characterizing Micro and Nanomaterials	
Symmetry in Crystallography	53	Using MEMS Technology	445
Sample Preparation for Metallography	66	THERMAL ANALYSIS	461
Atomic Excitation Exploited by Energetic-Beam		Thermal Analysis, Introduction	463
Characterization Methods	74	Principles and Practices of Thermal	
Particle Scattering	90	Analysis and Calorimetry	463
Combining Data from Multiple Techniques	105	Thermogravimetric Analysis	471
COMPUTATION AND THEORETICAL METHODS	113	Differential Scanning Calorimetry and	
Computation and Theoretical		Differential Thermal Analysis	483
Methods, Introduction	115	Combustion Calorimetry	496
Introduction to Computation	115	Thermal Diffusivity by the Laser Flash Technique	510
Bonding in Metals	119	Simultaneous Techniques Including Analysis of	
Summary of Electronic Structure Methods	131	Gaseous Products	517
Magnetism in Alloys	147	High-Temperature Drop Calorimetry	530
Multiscale Computational Characterization	174	Semiadiabatic (Isoperibol) Solution Calorimetry	540
Handling Time and Temperature in Materials		ELECTRICAL AND ELECTRONIC MEASUREMENT	551
Simulation	183	Electrical and Electronic Measurement,	
Prediction of Phase Diagrams	193	Introduction	553
Simulating Microstructural Evolution		Conductivity Measurement	554
Using the Phase Field Method	216	Hall Effect and Conductivity Measurements in	
Challenges to Structure Prediction and Structure		Semiconductor Crystals and Thin Films	564
Characterization at the Nanoscale	249	Capacitance-Voltage (C-V) Characterization of	
Molecular-Dynamics Simulation of Surface		Semiconductors	579
Phenomena	253	Deep Level Transient Spectroscopy	590
Binary and Multicomponent Diffusion	265	Impedance Spectroscopy of Dielectrics	
Simulation of Chemical Vapor		and Electronic Conductors	603
Deposition Processes	280	Electrical Measurements on Superconductors	
Kinematic Diffraction of X-Rays	298	by Transport	616

Measuring the Electronic Properties of Materials at the Nanoscale	636	Cyclotron Resonance	1245
Characterization of <i>pn</i> Junctions	652	Mössbauer Spectrometry	1259
Carrier Lifetime: Free Carrier Absorption, Photoconductivity, and Photoluminescence	658	NMR Spectroscopy in the Solid State	1280
		Nuclear Magnetic Resonance: Basic Principles and Liquid State Spectroscopy	1295
		Applications of Ferromagnetic Resonance	1316
MAGNETISM AND MAGNETIC MEASUREMENT	693	X-RAY TECHNIQUES	1337
Magnetism and Magnetic Measurement, Introduction	695	X-Ray Techniques, Introduction	1339
Generation and Measurement of Magnetic Fields	699	X-Ray Powder Diffraction	1340
Magnetic Moment and Magnetization	716	Pair Distribution Function Analysis	1361
Theory of Magnetic Phase Transitions	741	Single-Crystal X-Ray Structure Determination	1373
Magnetometry	745	X-Ray Diffraction and Spectroscopic Techniques for Liquid Surfaces and Interfaces	1393
Thermomagnetic Analysis	754	Surface X-Ray Diffraction	1424
Techniques to Measure Magnetic Domain Structures	766	Coherent Diffraction Imaging of Strain on the Nanoscale	1443
Magnetotransport in Metals and Alloys	780	X-Ray and Neutron Diffuse Scattering Measurements	1452
Surface Magneto-Optic Kerr Effect	793	XAFS Spectroscopy	1479
Magneto-Optical Characterization of Magnetic Thin Films, Surfaces, and Interfaces at Small Length and Short Time Scales	801	X-Ray Photoelectron Spectroscopy	1493
Magnetization Characterization of Superconductors	822	X-Ray Magnetic Circular Dichroism	1536
		Resonant Scattering Techniques	1556
		Resonant Inelastic X-Ray Scattering	1571
		Magnetic X-Ray Scattering	1580
		X-Ray Microprobe for Fluorescence and Diffraction Analysis	1607
		X-Ray Computed Tomography	1624
		High-Resolution 3D Imaging and Material Analysis with Transmission X-Ray Microscopy and Nano-CT	1642
		<i>In Situ</i> X-Ray Measurement Methods	1652
ELECTROCHEMICAL TECHNIQUES	833	ELECTRON TECHNIQUES	1673
Electrochemical Techniques, Introduction	835	Electron Techniques, Introduction	1675
Cyclic Voltammetry	837	Transmission Electron Microscopy	1675
Techniques for Corrosion Quantification	850	Scanning Electron Microscopy	1721
Semiconductor Photoelectrochemistry	864	Scanning Transmission Electron Microscopy: Z-Contrast Imaging	1736
Electrochemical Impedance Spectroscopy	898	<i>In Situ</i> TEM Measurement Methods	1764
Potentiostatic and Galvanostatic Intermittent Titration Techniques	913	Dynamic Transmission Electron Microscopy	1774
Microelectrodes	932	Lorentz Microscopy	1787
Scanning Electrochemical Microscopy	956	Fluctuation Electron Microscopy	1801
The Quartz Crystal Microbalance in Electrochemistry	968	Low-Energy Electron Microscopy	1808
		Spin-Polarized Low-Energy Electron Microscopy (SPLEEM)	1827
		Low-Energy Electron Diffraction	1841
		Energy Dispersive Spectrometry	1854
		Auger Electron Spectroscopy	1879
		Positron Annihilation Studies of Materials	1899
		Reflection High-Energy Electron Diffraction	1925
OPTICAL IMAGING AND SPECTROSCOPY	985	ION-BEAM TECHNIQUES	1939
Optical Imaging and Spectroscopy, Introduction	987	Ion-Beam Methods, Introduction	1941
Optical Microscopy	989	TOTAL IBA	
Reflected-Light Optical Microscopy	1010	“Total” Ion Beam Analysis – 3D Imaging of Complex Samples Using MeV Ion Beams	1948
Super-Resolution Optical Microscopy	1026		
Confocal Fluorescence Microscopy	1040		
Ultraviolet and Visible Absorption Spectroscopy	1054		
Raman Spectroscopy of Solids	1067		
Fourier Transform Infrared (FTIR) Spectroscopy	1104		
Ellipsometry	1135		
Ultraviolet Photoelectron Spectroscopy	1146		
Photoluminescence Spectroscopy	1158		
Dynamic Light Scattering	1170		
Impulsive Stimulated Thermal Scattering	1180		
RESONANCE METHODS	1197		
Resonance Methods, Introduction	1199		
Nuclear Magnetic Resonance Imaging	1200		
Nuclear Quadrupole Resonance	1214		
Electron Paramagnetic Resonance	1232		

Particle-Induced X-Ray Emission	1959	Phonon Studies	2205
Elastic Backscattering of Ions for Compositional Analysis	1974	Neutron Reflectometry	2226
Elastic Recoil Detection Analysis	1994	Small-Angle Neutron Scattering	2237
Nuclear Reaction Analysis (NRA) and Particle- Induced Gamma-Ray Emission (PIGE)	2006	Magnetic Neutron Scattering	2253
Low-Energy Ion Scattering	2024	SCANNING PROBE TECHNIQUES	2267
Medium-Energy Backscattering and Forward-Recoil Spectrometry	2044	Scanning Probe Microscopy Techniques, Introduction	2269
Secondary Ion Mass Spectrometry	2058	Scanning Tunneling Microscopy	2270
Scanning Helium Ion Microscopy	2091	Magnetic Sensitive Scanning Tunneling Microscopy	2280
Atom Probe Tomography and Field Ion Microscopy	2099	Atomic Force Microscopy and Spectroscopy	2290
Charged-Particle Irradiation for Neutron Radiation Damage Studies	2111	Magnetic Sensitive Scanning Probe Microscopy	2302
Radiation Effects Microscopy	2127	Electrostatic Force Microscopy and Kelvin Probe Force Microscopy	2310
Trace Element Accelerator Mass Spectrometry	2137	Scanning Near-Field Optical Microscopy	2321
NEUTRON TECHNIQUES	2163	Scanning Thermal Microscopy	2330
Neutron Techniques, Introduction	2165	Ultrasonic Atomic Force Microscopy	2340
Neutron Powder Diffraction	2165	INDEX	2351
Single-Crystal Neutron Diffraction	2192		

ELECTROCHEMICAL TECHNIQUES

7

ANDREW B. BOCARSLY, Chapter Editor

Department of Chemistry, Princeton University, Princeton, NJ, USA

Electrochemical Techniques, Introduction	835
<i>Andrew B. Bocarsly</i>	
Cyclic Voltammetry	837
<i>Andrew B. Bocarsly</i>	
Techniques for Corrosion Quantification	850
<i>Gerald S. Frankel</i>	
Semiconductor Photoelectrochemistry	864
<i>Samir J. Anz, Arnel M. Fajardo, William J. Royea, Nathan S. Lewis, and Amanda J. Morris</i>	
Electrochemical Impedance Spectroscopy	898
<i>Yevgen Barsukov and J. Ross Macdonald</i>	
Potentiostatic and Galvanostatic Intermittent Titration Techniques	913
<i>Mikhael D. Levi and Doron Aurbach</i>	
Microelectrodes	932
<i>Angela Molina and Joaquin Gonzalez</i>	
Scanning Electrochemical Microscopy	956
<i>Shigeru Amemiya</i>	
The Quartz Crystal Microbalance in Electrochemistry	968
<i>Georgia A. Arbuckle-Keil</i>	

Contents

ELECTROCHEMICAL TECHNIQUES, INTRODUCTION

Modern electrochemistry provides both a synthetic methodology to the materials scientist and an analytical tool for the evaluation of compositions and the kinetics of charge transfer processes. On the one hand, a variety of bulk materials and functional surfaces are prepared electrochemically. Historically this includes the electrorefining of materials such as aluminum, gold, and copper; surface preparation as illustrated in the anodization of aluminum, the electroetching of semiconductors, and the electroplating of thick metallic films. Similarly, the electrosynthesis of soft materials, for example, conducting organic polymers, is an important route in select cases. More recently, the electrosynthesis of quantum structures, either by direct deposition as in the case of ultra-thin film layered metal structures or by electroetching as exemplified in the synthesis of porous silicon, has become an important application of electrochemistry. On the other hand, electroanalytical chemistry has been developed as an extremely sensitive physical characterization technique for the quantification of conducting and semiconducting surfaces and interfaces. The corrosion properties/processes of metallic surfaces and semiconductor electronic properties are two key areas where electrochemical characterization has had high impact. In keeping with the central analytical theme of this work, this article limits its focus to the class of electrochemical techniques specifically aimed at characterizing materials and their interfaces (as opposed to synthetic electrochemistry). In some cases, the line between materials synthesis and measurement can become hazy. The field of sensors based on chemically modified electrodes (CMEs) is a good example of this confusion. Often sensors of this type are electrosynthesized and the synthesis parameters represent an important portion of the systems characterization. Cases such as this are included in the topical coverage of this article.

Electrochemistry differs from other analytical techniques in an important way. Unlike most instrumental characterization techniques, the sample under study is made into part of the measuring circuitry, and thus, inappropriate sample preparation can effectively lead to a malfunction of the instrument. This synergism between instrument and sample demands that the user have some knowledge of the detailed circuitry associated with the instrument being employed. While many instruments can be treated as "black boxes" where the user need only understand the rudiments of the instrument's functions, if this approach is employed in the execution of an electrochemical experiment, the result is often an artifactual instrument response that is easily misinterpreted as the chemical response of the sample. Unfortunately, the electrochemical literature repeatedly testifies to the preeminence of this problem, which has been made that much worse by modern instrumental

techniques that superimpose a computer interface between the user and the experiment.

Modern electroanalytical techniques have become viable characterization tools because of our ability both to precisely measure small currents and to mathematically model complex heterogeneous charge transfer processes. Detailed modeling of electrode-based charge transfer processes is best accomplished using digital simulation methods. There are presently several commercial software packages provided by the major potentiostat providers to this end. The mathematics and computer science related to this underpinning of electrochemistry is sophisticated and beyond the scope of this article. In most cases, an incomplete understanding of this aspect of electroanalysis will not affect the quality of the experimental outcome. In cases where the experimenter wishes to obtain a more detailed understanding of the physical chemical basis of electrochemistry, a variety of texts are available. Two volumes, the first by Bard and Faulkner (2001) and the second by Gileadi (1993) are particularly well-suited to a more detailed understanding of electrochemistry and electroanalysis. The latter volume is specifically aimed at the materials scientist, while the former work is one of the central texts in physical electrochemistry. A third text edited by Kissinger and Heineman (1996) is an excellent source of experimental details and analytical technologies. All these texts will be most valuable as supplements to this article, providing more chemical details but less materials-characterization emphasis than found here. In cases where specific data about the electrochemical behavior of an element or compound is required, it is typically necessary to consult the primary literature; however, an excellent starting point is the "Encyclopedia of the Electrochemistry of the Elements," edited by Bard (1973–1986).

Electrochemical measurements can be divided into two categories based on the required instrumentation. Potentiometric measurements utilize a sensitive voltmeter or electrometer and measure the potential of a sample against a standard of known potential. Voltammetric measurements utilize a potentiostat to apply a specified potential waveform to a sample and monitor the induced current response. Amperometric or galvanostatic measurements, in which the potential is held constant and the current monitored as a function of time, are included in this latter category. Potentiometric measurements form the historical basis of electrochemistry and are of present utility as a monitoring technique for solution-based processes (i.e., pH monitoring or selective ion monitoring). However, potentiometry is limited with regard to materials characterization. Thus, this article focuses on voltammetric measurements and the use of the potentiostat/galvanostat. The potentiostat is fundamentally a feedback circuit that monitors the potential of the test electrode (referred to as the working electrode) versus a reference half-cell (typically called a reference electrode). If the potential of the working electrode drifts from a prescribed offset potential versus the reference electrode, a correcting potential is applied. A third electrode, the counterelectrode (or auxiliary electrode), is present in the associated electrochemical cell to

complete the current pathway. The potentiostat typically contains a current-following circuit associated with the auxiliary electrode, which allows a precise determination of the current that is reported to a recording device as a proportional potential. The rudimentary operation of the potentiostat is covered in this article. However, for many applications a more detailed analysis of potentiostat electronics is desirable. To this end, the reader is directed to Kissinger and Heineman's volume (Kissinger and Heineman, 1996).

Potentiostats are available from a series of vendors and range in price from about \$1,000 to \$50,000. Almost all research-grade potentiostats today employ digital circuitry; thus, an external computer is required to carry out both control and data collection functions. Digital potentiostats have the major advantage that a wide variety of potential waveforms can be inexpensively preprogrammed giving the user access to a wide variety of experimental techniques. Typically, a decent quality digital potentiostat costs between \$11,000 and \$15,000. The price increases as specialized techniques requiring additional circuitry such as high-frequency AC impedance, rotating disk, or a bipotentiostat capability (i.e., two independently controlled working electrodes) are added. Although it is typical to advertise a potentiostat based on the number of techniques it can undertake along with the friendliness of the software, it is the size of the power supply utilized, the maximum slew (or step) rate of the unit, the dynamic stability of the circuitry, and the limiting current sensitivity that determines the quality of the instrument.

Material-based electrochemical investigations involve making the sample of interest into one electrode of an electrochemical cell. As such, it is immediately obvious that this technique is limited to materials having excellent to good conductivity. Inorganic metal samples and conducting organic polymers, therefore, immediately jump to mind as appropriate samples, and in this vein, issues related to the corrosion properties of the materials, the analytical composition of materials, and the electrocatalytic properties of materials are issues well-mated to electrochemical investigation. What may be less obvious is the application of electrochemical techniques to the characterization of semiconductor interfaces; however, this application is historically central to the development of electronic materials and continues to play a key role in semiconductor development to date; most recently the advent of organic semiconductor devices has been aided by electrochemical evaluation. Electrochemical investigation has played a key role in the development of junctions that both convert light to electrical energy and emit light, as well as control (switching) and sensing junctions.

The listing above points to obvious overlaps with other materials-characterization techniques and suggests complimentary strategies that may be of utility. In particular, the characterization of electronic systems using electrical circuit responses (see article ELECTRICAL AND ELECTRONIC MEASUREMENT) or electron spectroscopy (see article ELECTRON TECHNIQUES) is often combined with electrochemical characterization to provide a complete

picture of semiconducting systems. Thus, for example, one might employ solid-state electronics to determine the doping level or n-type versus p-type character of a semiconducting sample prior to evaluation of the sample in an electrochemical cell. Likewise, electron spectroscopy might be used to evaluate band-edge energetics or the nature of surface states in collaboration with electrochemical studies that determine interfacial energetics and kinetics. In passing, it is interesting to note that the first "transistor systems" reported by Bell Laboratories were silicon- and germanium-based three-electrode electrochemical cells (Brattain and Garrett, 1955). While these cells never met commercial requirements forcing the development of the solid-state transistor, these studies were critical in the development of our present understanding of semiconductor interfaces.

This article considers the most commonly utilized techniques in modern electrochemistry: polarography (i.e., currents induced by a slowly varying linear potential sweep), cyclic voltammetry (i.e., currents induced by a triangular potential waveform), and AC impedance spectroscopy (i.e., the real and imaginary current components generated in response to an AC potential of variable frequency). The characterization of semiconducting materials, the corrosion of metallic interfaces, and the general behavior of redox systems are considered in light of these techniques. In addition, the use of electrochemistry as a scanning probe microscopy technique for the visualization of chemical processes at conducting and semiconducting surfaces is also discussed. In the work presented here, the analytical power of electrochemistry is the focus, and the utility of electrochemistry as a synthetic tool is not as well developed. However, today electrochemical synthetic methodologies are playing a key role in the development of nanostructured materials, and the contribution by Arbuckle-Keil on the electrochemical quartz crystal microbalance highlights a key hybrid technique that brings together the synthetic and analytic abilities of modern electrochemistry.

LITERATURE CITED

- Brattain, W. H. and Garrett, C. G. B. 1955. *Bell System Tech.* 1.34:129.
- Bard, A. J. and Faulkner, L. R. 2001. *Electrochemical Methods, Fundamentals and Applications*, 2nd ed. John Wiley & Sons, New York.
- Gileadi, E. 1993. *Electrode Kinetics for Chemists, Chemical Engineers, and Materials Scientists*. VCH Publishers, New York.
- Kissinger, P. T. and Heineman, W. R. (eds.). 1996. *Laboratory Techniques in Electroanalytical Chemistry*, 2nd ed. Marcel Dekker, New York.
- Bard, A. J. editor. 1973–1986. *Encyclopedia of Electrochemistry of the Elements*, Volumes 1–15. Marcel Dekker, New York.

INTERNET RESOURCES

<http://lem.ch.unito.it/chemistry/electrochemistry.html>
An international umbrella web site at Università di Torino maintained by Carlo Nervi and Mauro Ravera. This site not only

covers electrochemistry at Torino (a major center), but has links to most other important electrochemical sites.

<http://electrochem.cwru.edu/estir/>

Web site of the Electrochemical Science and Technology Information Resource (EST/R), established by Zoltan Nagy at Case Western Reserve. This site is interfaced with a large quantity of electrochemical information and is an excellent resource point for the start of any search related to an electrochemical topic.

<http://www.electrochem.org/>

Web site of The Electrochemical Society.

<http://electroanalytical.org/>

Web site of the Society of Electroanalytical Chemistry, providing a full compliment of links to electrochemical sites.

<http://solarfuelshub.org/research-areas>

The Joint Center for Artificial Photosynthesis (JCAP) is the US Department of Energy's Hub for the development of materials (including nanomaterials) for the efficient conversion of sunlight to chemical fuels. This site highlights electrochemistry as it related to semiconductor electrodes, nanomaterials, and molecularly controlled interfaces.

ANDREW B. BOCARSLY

Department of Chemistry

Princeton University, Princeton, NJ, USA



CYCLIC VOLTAMMETRY

ANDREW B. BOCARSLY

Department of Chemistry, Princeton University,
Princeton, NJ, USA

INTRODUCTION

A system is completely characterized from an electrochemical point of view if its behavior in the three-dimensional (3D) space composed of current, potential, and time is fully specified. In theory, from such phenomenological data one can determine all the system's controlling thermodynamic and kinetic parameters, including the mechanism of charge transfer, rate constants, diffusion coefficients, standard redox potentials, electron stoichiometry, and reactant concentrations. A hypothetical $i(E, t)$ (current as a function of potential and time) dataset is shown in Figure 1. This particular mathematical surface has been synthesized using the assumption that the process of interest involves a reversible one-electron charge transfer. The term "reversible" is used here in its electrochemical sense, to indicate that charge transfer between the electrode and the redox-active species both is thermodynamically reversible—that is, the molecule(s) of interest can be both oxidized and reduced at potentials near the standard redox potential—and occurs at a rate of reaction sufficiently rapid that for all potentials where the reaction occurs, the process is never limited by charge-transfer kinetics. In such a case,

the process is completely described by the standard redox potential of the electrochemical couple under investigation, the concentration(s) of the couple components, and the diffusion coefficients of the redox-active species.

On the other hand, one can imagine a redox reaction that is totally controlled by the kinetics of charge transfer between the electrode and the redox couple. In this case, a different 3D current-potential-time surface is obtained that depends on the charge-transfer rate constant, the symmetry of the activation barrier, and the reactant concentrations. Of course, a variety of mechanisms in between these two extremes can also be obtained, each leading to a somewhat different 3D representation. In addition, purely chemical processes can be coupled to charge-transfer events, providing more complex reaction dynamics that will be reflected in the current-potential-time surface.

The enormous information content and complexity of electrochemical dynamics in the current-potential-time domain introduces two major experimental complications associated with electrochemical data. First is the pragmatic consideration of how much time is necessary to obtain a sufficiently complete dataset to allow for a useful analysis. The second, far more serious complication is that different charge-transfer mechanisms often translate into subtle changes in the $i(E, t)$ response. Thus, even after one has access to a complete dataset, visual inspection is typically an insufficient means to determine the mechanism of charge transfer. Furthermore, knowledge of this mechanism is critical to determining the correct approach to data analysis. Thus, given the requisite dataset, one must rely on a series of large calculations to move from the data to chemically meaningful parameters.

The approach described so far is of limited value as a survey tool, or as a global mechanistic probe of electrochemical phenomena. It is, however, a powerful technique for obtaining precise thermodynamic and kinetic parameters once the reaction mechanism is known. The mathematical resolution to the problem posed here is to consider the projection of the $i(E, t)$ surface onto a plane that is not parallel to the i - E - t axis system. This is the basis of cyclic voltammetry. Not surprisingly, a single projection is not sufficient to completely characterize a system; however, if judiciously chosen, a limited set of projections (on the order of a half dozen) will provide sufficient information to determine the reaction mechanism and obtain the key reaction parameters to relatively high precision. Perhaps more importantly, reduction of the data to two dimensions allows one to determine the mechanism based on pattern recognition, and thus no calculational effort is required. Practically, the projection of interest is obtained by imposing a time-dependent triangular waveform on the electrode as given by Equation 1:

$$E(t) = \begin{cases} E_i + \omega t & \text{for } 0 \leq t \leq t_i \\ E_i + \omega t_i - \omega t & \text{for } t_i \leq t \end{cases} \quad (1)$$

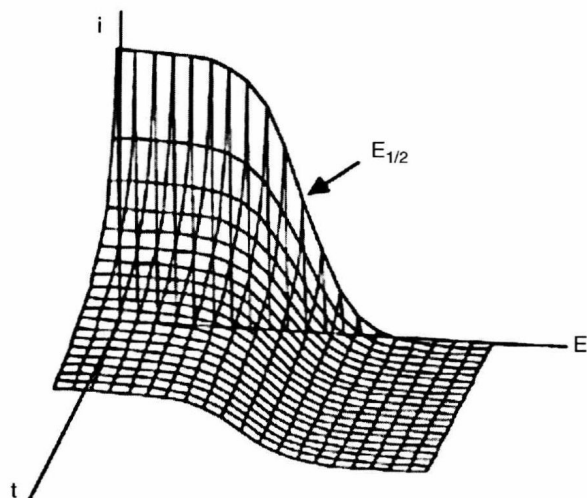


Figure 1. Theoretically constructed current-potential-time [$i(E,t)$] relation for an ideal, reversible, one-electron charge-transfer reaction taking place at an electrode surface. The half-wave potential, $E_{1/2}$, is the redox potential of the system under conditions where reactant and product diffusion coefficients are similar and activities can be ignored.

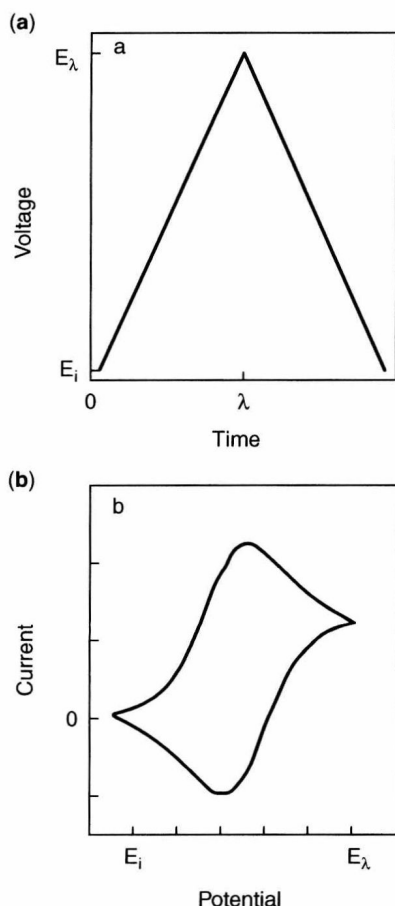


Figure 2. (a) Triangular $E(t)$ signal applied to the working electrode during a cyclic voltammetric scan. E_{λ} is the switching potential where the scan direction is reversed. (b) Cyclic voltammetric current versus potential response for an ideal, reversible one-electron redox couple under the $E(t)$ waveform described in (a).

where E_i is the initial potential of the scan, ω is the scan rate (in mV/s), and t_{λ} is the switching time of the triangular waveform as shown in Figure 2a. The induced current is then monitored as a function of the electrode potential as shown schematically in Figure 2b. The wave shape of the i - E plot is diagnostic of the mechanism. Different projection planes are simply sampled by varying the value of ω for a series of cyclic voltammetric scans. Although the 2D traces obtained offer a major simplification over the 3D plots discussed above, their chief power, as identified initially by Nicholson and Shain (1964), is that they are quantified from a pattern-recognition point of view by two easily obtained scan-rate-dependent parameters. Nicholson and Shain showed that these diagnostic parameters, peak current (s) and peak-to-peak potential separation, produce typically unique scan-rate dependencies as long as they are viewed over a scan-rate range that traverses at least 3 orders of magnitude. The details of this analysis are provided later. First, one needs to consider the basic experiment and the impact of laboratory variables on the results obtained.

The qualitative aspect of cyclic voltammetry has made it a general tool for the evaluation of electrochemical systems. With regard to materials specifically, the technique has found use as a method for investigating the electrosynthesis of materials (including conducting polymers and redox-produced crystalline inorganics), the mechanism of corrosion processes, the electrocatalytic nature of various metallic systems, and the photoelectrochemical properties of semiconducting junctions. Here a general description of the cyclic voltammetric technique is provided along with some examples focusing on materials science applications.

PRINCIPLES OF THE METHOD

Reaction Reversibility

The Totally Reversible Reaction. The simplest charge-transfer mechanism to consider is given by Equation 2, a reversible redox process:



For this process, the concentration of the reactant and products at the electrode surface is given by the Nernst equation (Equation 3) independent of reaction time or scan rate:

$$E = E_R - (2.303) \frac{RT}{nF} \log \frac{[\text{Red}]}{[\text{Ox}]} \quad (3)$$

where E is the electrode potential, E_R is the standard redox potential of the redox couple, $[\text{Red}]$ and $[\text{Ox}]$ are the concentrations of the reduced and oxidized species, respectively, R is the gas constant, T is the temperature (K), F is Faraday's constant, and n is defined by Equation 2. [At room temperature, 298 K, $2.303 (RT/nF) = 59 \text{ mV}/n$.] Equation 3 indicates that the electrode

potential, E , is equal to the redox couple's redox potential, E_R , when the concentrations of the oxidized species and reduced species at the electrode/electrolyte interface are equal. It can be shown that this situation is approximately obtained when the electrode is at a potential that is halfway between the anodic and cathodic peak potentials. This potential is referred to as the cyclic voltammetric half-wave potential, $E_{1/2}$. More precisely it can be demonstrated that the half-wave potential and the standard redox potential are related by Equation 4:

$$E_{1/2} = E_R - \frac{RT}{nF} \ln \left(\frac{\gamma_{\text{Ox}}}{\gamma_{\text{Red}}} \left[\frac{D_{\text{Red}}}{D_{\text{Ox}}} \right]^{1/2} \right) \quad (4)$$

where D_{Ox} and D_{Red} are the diffusion coefficients of the oxidized and reduced species, respectively, and the γ values represent the activity coefficients of the two halves of the couple. While this result is intuitively appealing, a solid mathematical proof of the relationship is complex and beyond the scope of this unit. The mathematical details are well presented in a variety of textbooks, however (Gileadi et al., 1975; Bard and Faulkner, 2001; Gossner, 1993).

By its very nature, the reversible redox reaction cannot cause a substantial change in the connectivity or shape of a molecular system. As a result, the diffusion coefficients of the oxidized and reduced species are expected to be similar, as are the activity coefficients—in which case Equation 4 reduces to $E_{1/2} = E_R$. Even if there is some variation in the diffusion coefficients, the square root functionality invariably produces a ratio close to 1, and thus the second term in Equation 4 can safely be ignored. Likewise, at a low concentration of electroactive species (as is typically employed in cyclic voltammetry), the activity coefficients can safely be ignored. Once a system has been demonstrated to be reversible (or quasireversible, as discussed later), the redox potential can then be directly read off the cyclic voltammogram.

For the reversible mechanism, the idealized cyclic voltammetric response is illustrated in Figure 2b. Within the context of the Nicholson and Shain diagnostic criteria, this cyclic voltammetric response provides a coupled oxidation and reduction wave separated by $\sim 60/n\text{mV}$ independent of the scan rate. The exact theoretical value for the peak-to-potential separation is not critical since this value is based on a Monte Carlo approximation and is somewhat dependent on a variety of factors that are often not controlled. In a real electrochemical cell, the ideal value is typically not achieved. The peak height of the anodic and cathodic waves should be equivalent, and the current function (for either the anodic or cathodic waves) is expected to be invariant with scan rate. Under such conditions the peak current is given by Equation 5 (Bard and Faulkner, 2001):

$$i_p = (2.69 \times 10^5) n^{3/2} A D_0^{1/2} \omega^{1/2} C_0 \quad (5)$$

where n is as defined by Equation 3, A is the area of the working electrode in cm^2 , D_0 is the diffusion coefficient of the electroactive species having units of cm^2/s , ω is the scan rate in mV/s , and C_0 is the bulk electrolyte concentration in moles/cm^3 . (Note that these are not the standard units of concentration.)

One important caveat must be noted here: the peak-to-peak separation is not solely dependent on the charge-transfer mechanism; cell resistances, for example, will increase the peak-to-peak separation beyond the anticipated $60/n\text{mV}$. Thus, the practical application of the diagnostic is a constant small peak-to-peak separation ($\sim 100/n\text{mV}$) with scan rate. It is also important to realize that the impact of cell resistance on potential ($V = iR$) is scan-rate-dependent since the magnitude of the observed current increases with scan rate. Thus, under conditions of high cell resistance (e.g., when a nonaqueous electrolyte is used), a reversible couple may yield a scan-rate-dependent peak-to-peak potential variation significantly greater than the ideal $\sim 60\text{-mV}$ shift. It is therefore critical to evaluate all three of the diagnostics over a reasonable range of scan rates before reaching a mechanistic conclusion.

The Totally Irreversible Reaction. The opposite extreme of a reversible reaction is the totally irreversible reaction. As illustrated by Equation 6, such a reaction is kinetically sluggish in one direction, producing a charge-transfer-limited current. The reaction is assigned a rate constant k ; however, it is important to note that k is dependent on the overpotential, η , where η is the difference between the redox potential of the couple and the potential at which the reaction is being observed ($E_R - E_{\text{electrode}}$). It is convenient to define a heterogeneous charge transfer rate constant, k_s , which is the value of k when $\eta = 0$.



For this case, a mass transport-limited current is only achieved at large overpotentials, since the rate constant for charge transfer is small for reasonable values of the electrode potential. The concentrations of redox species near the electrode are never in Nernstian equilibrium. Thus, one cannot determine either the redox potential or the diffusion coefficients associated with this system. However, careful fitting of the cyclic voltammetric data can provide the heterogeneous charge-transfer rate constant, k_s , and activation-barrier symmetry factor as initially discussed by Nicholson and Shain (1964) and reviewed by Bard and Faulkner (2001; Gossner, 1993). In the case of a very small value of k_s , the irreversible cyclic voltammogram is easily identified, since it consists of only one peak independent of the scan rate employed. This peak will shift to higher potential as the scan rate is increased. For moderate but still limiting values of k_s one will observe a large peak-to-peak separation that is scan-rate dependent. The $E_{1/2}$ value will also vary with scan rate. In this case, it is important to rule out unexpected cell resistance as the source of the potential dependence, before concluding that the reaction is irreversible. Often

modern digital potentiostats are provided with software that allows the direct measurement (and real time correction) of cell resistance via a current-interrupt scheme in which the circuit is opened for a short (millisecond) time period and the cell voltage is measured. Analog potentiostats often have an iR compensation circuit (Kissinger and Heineman, 1996).

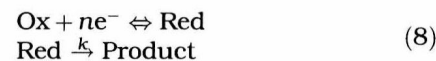
The Quasireversible Reaction. Although arbitrary, it is practically useful to define reversible charge-transfer systems as those having a heterogeneous charge-transfer rate constant in excess of $0.3\omega^{1/2}$, while totally irreversible systems are those exhibiting rate constants less than $2 \times 10^{-5}\omega^{1/2}$. (Note that this definition is quite surprising in that the requisite minimum rate constant for a reversible reaction depends on the potentiostat being employed. As the slew rate of the system increases, the ability to see large charge-transfer rate constants is enhanced. This is unfortunate, in that it clouds the distinction between thermodynamics and kinetics). This definition produces a large number of reactions having intermediate rate constants ($0.3\omega^{1/2} \geq k_s \geq 2 \times 10^{-5}\omega^{1/2}$), which are referred to as quasireversible systems. These systems will appear reversible or irreversible depending on the scan rate employed. For sufficiently large scan rates, the rate of interfacial charge transfer will be limiting and the system will appear irreversible. For slower scan rates, the system response time will allow the Nernst equation to control the interfacial concentrations and the system will appear reversible. Depending on the scan rate employed, one can determine systemic thermodynamic parameters (redox potential, n , and diffusion coefficient) or kinetic parameters. As in the reversible case, the current function for quasireversible systems tends to be scan rate independent. The peak-to-peak potential dependence is also often an inconclusive indicator. However, the potential of the peak current(s) as a function of scan rate is an excellent diagnostic. At low scan rates, the peak potential can approach the theoretical $\sim 30/n\text{mV}$ separation from the half-wave potential in a scan rate-independent manner; however, as the scan rate is increased and the system enters the irreversible region and the peak potential shifts with $\log \omega$. This dependence is given by Equation 7 (Gileadi, 1993):

$$E_p^{\text{irr}} = E_{1/2} - \sigma \left[0.52 + \log \left(\frac{D\omega}{\sigma} \right)^{1/2} - \log k_s \right] \quad (7)$$

where σ is the Tafel slope, a measure of the kinetic barrier, and the other terms are as previously defined. Note that the slope of E_p versus $-0.5 \log \omega$ allows one to determine (σ/D) , while D and $E_{1/2}$ can be obtained from cyclic voltammograms taken in the reversible region allowing one to determine $k(E_{1/2})$ (see Fig. 5c for an example of this type of behavior).

Nonreversible Charge-Transfer Reactions. In contrast to mechanistically "irreversible reactions," which indicate

a kinetic barrier to charge transfer, a mechanistically "nonreversible reaction" refers to a complex reaction mechanism in which one or more chemical steps are coupled to the charge-transfer reaction (Nicholson and Shain, 1965; Polcyn and Shain, 1966a,b; Saveant, 1967a,b; Brown and Large, 1971; Andrieux et al., 1980; Bard and Faulkner, 2001; Gosser, 1993; Rieger, 1994). For example, consider the generic chemical reaction shown as Equation 8:



where k represents the rate constant for a non-electrochemical transformation such as the formation or destruction of a chemical bond. This reaction couples a follow-up chemical step to a reversible charge-transfer process and is thus referred to as an EC process (electrochemical step followed by a chemical step). Consider the effect of this coupling on the cyclic voltammetric response of the Ox/Red system. At very fast scan rates, Ox can be converted to Red and Red back to Ox before any appreciable Product is formed. Under these conditions, the Nicholson and Shain diagnostics will appear reversible. However, as the scan rate is slowed down, the redox couple will spend a longer time period in the Red state and thus the formation of Product will diminish the amount of Red below the "reversible" level. Therefore, at slow scan rates the ratio of peak currents (i_a/i_c) will increase above unity (the reversible value). On the other hand, the current function for the cathodic current will decrease below the reversible level as Red is consumed and thus becomes unavailable for back-conversion to Ox. The peak-to-peak potential is not expected to change for the mechanistic case presented. This set of diagnostics is unique and can be used to demonstrate the presence of an EC mechanism. Likewise, one can consider mechanisms where a preliminary chemical step is coupled to a follow-up electrochemical step (a CE mechanism) or where multiple chemical and electrochemical steps are coupled. In many of the cases that have been considered to date, the Nicholson and Shain diagnostics provide for a unique identification of the mechanism if viewed over a sufficiently large scan-rate window. An excellent selection of mechanisms and their expected Nicholson and Shain diagnostics are presented in Brown and Large (1971).

PRACTICAL ASPECTS OF THE METHOD

Since a cyclic voltammetric experiment is fundamentally a kinetic experiment, the presence of a well-defined internal "clock" is essential. That is, the time dependence is provided experimentally by the selected scan rate since the input parameter $E(t)$ is implicitly a time parameter. However, in order for this implicit time dependence to be of utility it must be calibrated with a chemically relevant parameter. The parameter used for this purpose

is the diffusion of an electroactive species in the electrolyte. Thus, the cyclic voltammetric experiment is fundamentally a "quiet" experiment in which convective components must be eliminated and the diffusion condition well defined. This is done by considering the geometry of the electrochemical cell, the shape of the electrode under investigation, and the time scale of the experiment.

Additionally, from the essence of the experiment, the application of an electrode potential combined with the monitoring of the induced current, it is important to know to high precision the time-dependent electrode potential function, $E(t)$, for all values of t . This capability is established by using a potentiostat to control an electrochemical cell having a three-electrode cell configuration. Successful interpretation of the electrochemical experiment can only be achieved if the experimenter has a good knowledge of the characteristics and limitations of the potentiostat and cell configuration employed.

Electrochemical Cells

Cyclic voltammetric experiments employ a "three-electrode" cell containing a working electrode, counterelectrode (or auxiliary electrode), and reference electrode. The working electrode is the electrode of interest; this electrode has a well-defined potential for all values of $E(t)$. The counterelectrode is simply the second electrode that is requisite for a complete circuit. The reference electrode is in fact not an electrode at all, but rather an electrochemical half-cell used to establish a well-defined potential against which the working electrode potential can be measured. Typically, a saturated calomel electrode (SCE—a mercury-mercurous couple) or a silver-silver chloride electrode is utilized for this purpose. Both of these reference half-cells are commercially available from standard chemical supply houses. While the consideration of reference half-cells is important to any electrochemical experiment, it is beyond the scope of this unit; the reader is referred to the literature for a consideration of this topic (Gileadi, 1993; Gosser, 1993; Rieger, 1994). The exact geometry of the three electrodes, along with the shape and size of the working electrode, will determine the internal cell resistance and capacitance. These electrical parameters will provide an upper limit for both the current flow (via Ohm's law: $i = V/R$, where V is voltage and R is resistance) and the cell response time (via the capacitive time constant of the cell). The contact between the reference half-cell and the remainder of the electrochemical cell is typically supplied through a high-impedance frit, ceramic junction, or capillary. A high-impedance junction is employed for two purposes: to eliminate chemical contamination between the contents of the reference electrode electrolyte and the electrolyte under investigation and to guarantee a minimal current flow between the reference and working electrodes; the voltage drop associated with this current, referred to as iR drop (Ohm's law), is uncompensated by standard potentiostat circuitry. If this voltage drop becomes substantial (see Equation 9 and discussion below), the data will be highly

distorted and not representative of the chemical thermodynamics/kinetics under investigation.

Potentiostats and Three-Electrode Electrochemical Cells

At its heart, the potentiostat is a negative-feedback device that monitors the potential drop between the working electrode and the reference electrode. If this value deviates from a preselected value, a bias is applied between the working and counterelectrodes. The working/counterelectrode voltage drop is increased until the measured working electrode versus reference electrode potential returns to the preset value (Gileadi et al., 1975; Gileadi, 1993). In order to carry out a cyclic voltammetric experiment, a potential waveform generator must be added to the potentiostat. The waveform generator produces the potential stimuli presented by Equation 1. Depending on the instrument being utilized, the waveform generator may be internal to the instrumentation or provided as a separate unit.

The cyclic voltammetric "figure of merit" of a potentiostat will depend on the size of the power supply utilized and the rise time (or slew rate) of the power supply. The rise time determines the maximum scan rates that can be used in fashioning the $E(t)$ waveform. In addition to the power-supply slew rate, the cell requirements of a nonconvective system coupled with practical limits at which the potential of the working electrode can be varied (due to the resistance-capacitance (RC) time constant associated with a metal/electrolyte interface) provide upper and lower limits for the accessible scan-rate range. Unless the cell is carefully insulated from the environment, thermal and mechanical convective currents will set in for scan rates much below $\sim 1\text{--}2\text{ mV/s}$; this establishes a practical lower limit for the scan rate. The upper limit is dependent on the size of the electrode and the resistance of the cell. For typical cyclic voltammetric systems (electrode size $\sim 1\text{ mm}^2$), scan rates above $\sim 10\text{ V/s}$ tend to introduce complications associated with the cell RC time constant. However, scan rates as high as $100,000\text{ V/s}$ have been reported in specially engineered cells employing ultramicroelectrodes and small junction potentials. More realistically, careful limitation of cell resistance allows one to achieve maximum scan rates in the $10\text{--}100\text{ V/s}$ range.

The size of the power supply determines the potentiostat compliance voltage (the largest voltage that can be applied between the working and counterelectrodes). This voltage determines the potentiostat's ability to control the potential of the working electrode. If one is working in a single-compartment cell with an aqueous electrolyte containing a relatively high salt concentration (≥ 0.1 molar salt), then a relatively modest power supply ($\sim 10\text{ V}$) will provide access to all reasonable working electrode potentials. However, in order to carry out cyclic voltammetric studies in high-resistance cells (i.e., those with low salt concentrations, multiple electrochemical compartments, and/or nonaqueous electrolytes) a compliance voltage on the order of 100 V may be required. It is extremely important to note when using a high-compliance voltage potentiostat that the potential reported by

the potentiostat is the voltage drop between the reference electrode and the working electrode. Although this value will never exceed ~ 3 V, in order to achieve this condition, the potentiostat may have to apply ~ 100 V between the counter and working electrodes. *Since the leads to these electrodes are typically exposed, the researcher must use utmost care to avoid touching the leads, even when the potentiostat is reporting a low working electrode potential. If the experimenter is accidentally inserted into the circuit between the working and counterelectrodes, the full output voltage of the power supply may run through the experimenter's body.*

In order to determine the potential of the working electrode with regard to the reference electrode, the potentiostat employs an electrometer. The value measured by the electrometer is used both to control the potentiostat feedback loop and to produce the potential axis in the cyclic voltammogram. As such it is assumed that the electrometer reading accurately reflects the potential of the working electrode, ϕ . In fact, the electrometer reading, E_{obs} , is better represented by Equation 9:

$$E_{\text{obs}} = \phi + iR \quad (9)$$

where iR is the uncompensated voltage drop between the working and reference electrodes. In general, application of a voltage between two electrodes (in this case, the working and reference) may cause a current to flow. This would result in a large value for the iR term (and be deleterious to the reference half cell). This problem is circumvented by employing a high-impedance junction between the working electrode and reference electrode, as noted earlier. This junction ensures that the value of i will be quite small and thus iR will have a small value. In this case $E_{\text{obs}} \approx \phi$ and the potentiostat reading is reliable. However, if R is allowed to become excessively large, then even for a small value of i , the iR term cannot be ignored, and an error is introduced into the cyclic voltammogram. High scan rates produce large peak currents, not only exacerbating the iR drop but introducing a phase-lag problem associated with the cell's RC time constant. Both these effects can severely distort the cyclic voltammogram. If this occurs, it can be remedied by switching to a low-impedance reference electrode. Decreasing the cell R improves both the iR and RC responses at the cost of destabilizing the potential of the reference half-cell.

The Working Electrode

The working electrode may be composed of any conducting material. It must be recognized that the shape, area, and internal resistance of this electrode affect the resulting current (Nicholson and Shain, 1964; Bard and Faulkner, 2001; Kissinger and Heineman, 1996), and therefore these parameters must be controlled if the cyclic voltammetric data is to be used analytically. Almost all the kinetic modeling that has been carried out for cyclic voltammetric conditions assumes a semi-infinite linear-diffusion paradigm. In order to meet

this condition, one needs a relatively small electrode ($\sim 1 \text{ mm}^2$) that is planar. The small size assures low currents. This both limits complications associated with iR drop and provides well-defined diffusion behavior. If the above conditions cannot be met, then a correction factor can be employed prior to data analysis (Kissinger and Heineman, 1996).

In cases where cyclic voltammetric studies are applied to solution species, typical working electrode materials include platinum, gold, mercury, and various carbon materials ranging from carbon pastes and cloths to glassy carbon and pyrolytic graphite. These materials are selected because they are inert with respect to corrosion processes under typical electrochemical conditions. A second selection criteria is the electrode material's electrocatalytic nature (or lack thereof). Platinum, broadly speaking, presents a catalytic interface. This is particularly true of reactions involving the hydrogen couple. As a result, this material is most often utilized as the counterelectrode, thereby ensuring that this electrode does not kinetically limit the observed current. For the same reasons, platinum tends to be the primary choice for the working electrode. The other materials noted are employed as working electrodes because they either are electrocatalytic for a specific redox couple of interest, provide exceptional corrosion inertness in a specific electrolyte of interest, or present a high overpotential with respect to interfering redox couples. With respect to this latter attribute, carbon and mercury are of interest, since both have a high overpotential for proton reduction. As such, one can access potentials significantly negative of the water redox potential in aqueous electrolyte using a carbon or mercury working electrode. Typically, potentials that are either more negative than the electrolyte reduction potential or more positive than the electrolyte oxidation potential are not accessible, since the large current associated with the electrolysis of the electrolyte masks any other currents. Carbon also presents an interesting interface for oxidation processor in aqueous electrolytes since it also has a high overpotential for water oxidation. Mercury, on the other hand, is not useful at positive potentials since it is not inert in this region, oxidizing to Hg^{2+} . In addition to standard metal-based electrodes, a variety of cyclic voltammetric studies have been reported for conducting polymer electrodes, semiconducting electrodes, and high- T_c superconducting electrodes.

An alternate basis for selecting an electrode material is mechanical properties. For example, the mercury electrode is a liquid electrode obtained by causing mercury to flow through a glass capillary. The active electrode area is at the outlet of the capillary, where a droplet of mercury forms, expands, and eventually drops off. This has two major electrochemical consequences. First, the electrode surface is renewed periodically (which can be helpful if surface poisoning by solutions species is an issue); second, the area of the electrode increases in a periodic manner. One can control (as a function of time) the electrode area and lifetime by controlling the pressure applied to the capillary. Obviously, this type of control is not available when using a solid electrode.